Mohammed A. Rzooqi [1]
Rayan T. Al Douri [2]
Qahtan N. Abdullah [3]
Abdullah Alaliaan [4]
Abdulkareem A. Hussain [5]
Sundus M. Meteab [6]

Characterization of Nanocomposites SnO_2:Cu for Gas Sensing Applications

The paper discusses the importance of improving and developing gas sensors, with a special focus on tin oxide nanoparticles doped with Cu nanoparticles for NO_2 detection. The structural, morphological and optical properties of the SnO_2 nanofilms were revealed using XRD, FE-SEM and UV-Vis characterization. The structure of the material was attributed to the tetragonal crystalline configurations of SnO_2. With the enhancement of Cu doping, the absorbance decreased with an increase in the optical bandgap values from 3.02 to 3.28 eV. An increase in the sensitivity values to nitrogen dioxide gas was reported for the films prepared from pure SnO_2 and incorporated with Cu nanoparticles at 2.4 wt%, where the sensitivity increased with increasing operating temperature and doping ratios for three temperatures (50, 100, 150) °C. For the pure SnO2 sample, the sensitivity increased from 1.8% and then increased upon adding Cu nanoparticles to 105% at 150 °C, which is the highest degree reported previously.

Keywords: Nanocomposites; Gas sensing; Tin dioxide; Copper dopants
Received: 11 January 2025; **Revised:** 4 March; **Accepted:** 11 March 2025

[1] Ministry of Education, General Directorate of Salah al-Din Education, Vocational Education Department, Dour, IRAQ
[2] Ministry of Education, General Directorate of Salah al-Din Education, Al-Dour Education Department, Dour, IRAQ
[3] Department of Physics, College of Education for Pure Sciences, University of Tikrit, Tikrit, IRAQ
[4] Department of Physics, College of Education for Pure Sciences, University of Samarra, Samarra, IRAQ
[5] Ministry of Education, General Directorate of Salah al-Din Education, Samarra Education Department, Samarra, IRAQ
[6] Department of Physics, College of Education for Pure Sciences, University of Anbar, Anbar, IRAQ

1. Introduction

The rising population, industrialization, vehicles, air conditioning units, and other sources contribute to the emission of several gases, adversely impacting the environment. Investigations are underway to identify and alleviate harmful gasses. Emissions from fossil fuel combustion, automotive emissions from internal combustion, and explosions have prompted the advancement of innovative sensing techniques [1-4]. Semiconductor materials are extensively studied in gas sensors owing to their durability and superior performance. In gas-sensing applications, the structure of semiconductor materials and surface modification are crucial. Numerous creative methods leveraging the optical and optoelectronic characteristics of these materials are achieving broad popularity [5,6]. The "solid-gas" interactions transpire on the surfaces of metal oxide semiconductors (MOS) at elevated temperatures ranging from 100 to 300 °C. This temperature is essential to enhance the concentration of free charge carriers, activate surface chemical processes, and facilitate desorption of reaction products. The requirement for heating significantly elevates the power consumption of semiconductor sensors, hence constraining their application in standalone and portable devices, particularly in communication systems such as smartphones. Upon the detection of oxidizing gas (NO_2), sensor signal production transpires due to the adsorption of analyte molecules on the metal oxide surface, resulting in the localization of electrons on the adsorbed species, which diminishes the electrical conductivity (for n-type semiconductors) [7-14]. Tin dioxide (SnO_2), a globally recognized n-type multifunctional semiconductor, possesses a broad straight bandgap energy of 3.6 eV at 300 K. Moreover, due to the substantial length-to-diameter and surface-to-volume ratios at the nanoscale, the gas sensing and optoelectronic characteristics of one-dimensional SnO_2 and nanostructures exhibit heightened sensitivity to adsorbed species on their surfaces [15]. SnO_2:Cu nanocomposites have elevated electron conductivity and mobility, demonstrating significant applications in transparent electrodes for solar cells [16], anode materials [17], and sensors [18]. The amalgamation of metal (Cu) with tin dioxide (SnO_2) presents a viable strategy for augmenting the physical and chemical attributes of nanocomposites [19]. Copper nanoparticles are highly desirable because to their substantial natural abundance, affordability, and superior catalytic, optical, electrical, and mechanical properties [20]. The gas sensor used in this study was manufactured from SnO_2 metal oxide and doped with (2 and 4%) copper nanoparticles using spray pyrolysis (CSP). We used a comb-type aluminum metal contact for the tool. The optical, structural and microscopic properties of the sample were analyzed to obtain additional information regarding its shape, purity and other properties. Gas sensing measurements were performed, and their selectivity and sensitivity along with different response and recovery rates were

evaluated.

2. Experimental Part

Initially, two types of solutions were prepared, the first solution was tin chloride ($SnCl_2.2H_2O$) was used, its molecular weight (225.65 g/mol) and prepared by with a 99% purity. The solution was prepared at a molar concentration of 0.02 M. A 0.4513 g of tin $SnCl_2.2H_2O$ was dissolved in 100 ml of deionized water, then the solution was mixed using a magnetic stirrer for 30 min and after completing the dissolution process, we filtered the solution Using special filter papers to make the solution ready for spraying. As for the second solution, the copper was prepared. To prepare it, copper chloride ($CuCl_2.2H_2O$) with a molecular weight of 170.48 g/mol and prepared by Alpha Chemika Company with 99% purity was used. The solution was prepared at a molar concentration of 0.02 mol/L. A 0.34096 g of $CuCl_2$:$2H_2O$ was dissolved in 100 ml of deionized water and then added in different percentage volume ratios (0.02 and 0.04) to the aqueous tin dioxide chloride solution.

To fabricate the gas sensor shown in Fig. (1), aluminum (Al) electrodes were coated on the surface of the thin nanostructures produced using the CVD technique. The pressure in the deposition chamber was reduced to 0.1 mbar, and the Al electrodes were evaporated using a comb-shaped multifinger mask to create the metal-semiconductor-metal (MSM) sensor.

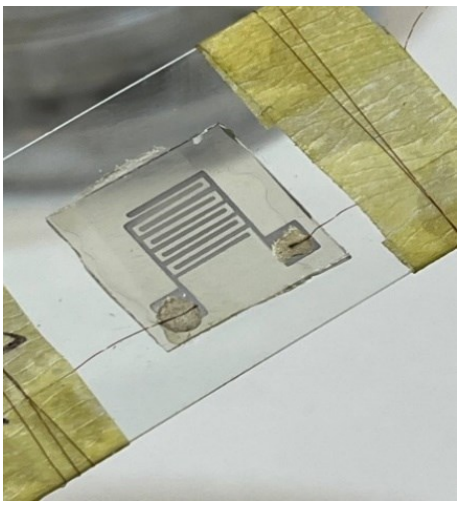

Fig. (1) Photograph of a SnO_2:Cu nanocomposite gas sensor device fabricated in this work

3. Results and Discussion

The phase purity and crystalline structure of the produced nanomaterial were examined using x-ray diffraction (XRD). This verifies that the SnO_2 structure is tetragonal. These correspond with the standard JCPDS card no. 01-077-0452. In Fig. (2), the presence of several peaks is observed in the XRD pattern belonging to pure SnO_2 and doped with Cu (2 and 4 %), at 2θ = 26.31°, 33.60°, 37.77°, 51.67°, and 64.23°, corresponding respectively to the crystal planes of (110), (101), (111), (211) and (112), with preferred orientation of plane (110).

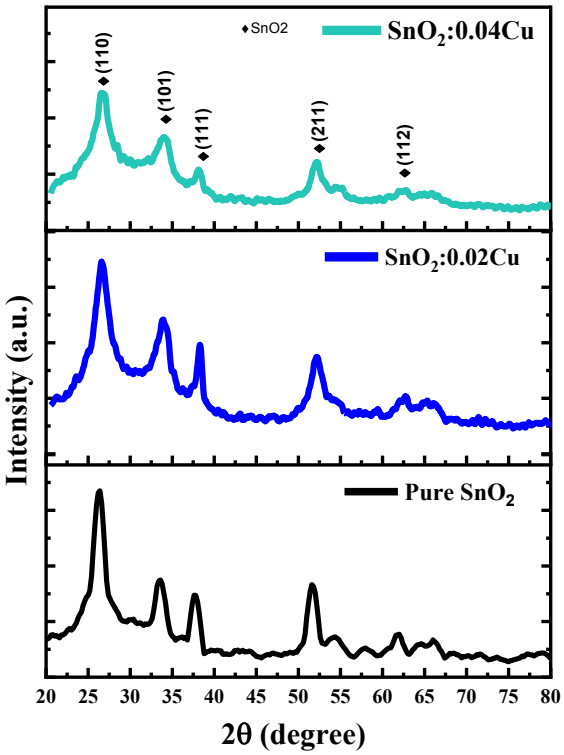

Fig. (2) XRD patterns of (a) pure SnO_2, (b) SnO_2:0.02 Cu and (c) SnO_2:0.04 Cu

The crystallite size (D) of the pure SnO_2 and doped with Cu nanoparticles was calculated using Debye-Scherrer's equation, expressed by [21]:

$$D = \frac{0.9\lambda}{\beta cos\theta} \quad (1)$$

where β is the full-width at half maximum (FWHM) of the peak and θ is the Bragg's angle

As can be seen from table (1), there is a variation in the crystallite size when copper ions (Cu^{2+}) are added to the SnO_2 lattice, as they can replace tin atoms (Sn^{4+}) in the crystalline structure. This substitution leads to changes in the crystalline structure such as increasing the regularity of the crystal due to the difference in ionic size between Cu^{2+} and Sn^{4+}. These changes can improve the crystal growth and reduce the structural defects, resulting in an increase in the average size [22].

In order to analyze the surface morphology of SnO_2:Cu thin films, field-emission scanning electron microscopy (FE-SEM) was used. Figure (3a) shows that the particles are well connected to each other. The surface of the film is heterogeneous and porous, which makes it more sensitive to gases. The average particle size of the pure film was determined to be 76.44 nm. The SnO_2 doped with 2% and 4% Cu nanoparticles, as shown in figures (3b) and (3c), shows that increasing the doping ratio changes the shape and size of the

particles to a hemispherical shape.

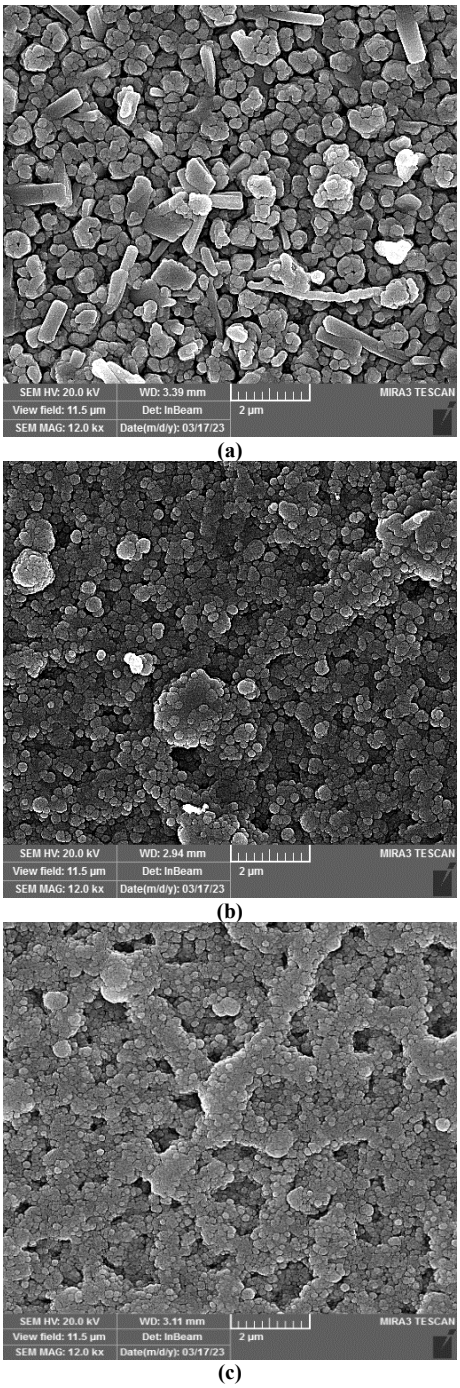

Fig. (3) FE-SEM images of (a) pure SnO_2, (b) SnO_2:0.02 Cu and (c) SnO_2:0.04 Cu

The particles are connected to each other to form aggregated clusters, which are further connected to larger particles randomly distributed across the film surface. The particle size decreases, reaching 38.47 nm at 2% and 25.35 nm at 4%. It is noted that as the percentage of inoculation increases, the shape and size of the granules change to become semi-spherical, as the granules are linked to each other to form clusters of clusters, and these clusters are linked to other large granules, which are randomly distributed on the surface of the film. The surface texture is rough for the 4% sample, as each crack-like structure consists of smaller nanoparticles or crystalline faces.

The UV-visible absorption spectra of the prepared Cu-doped SnO_2 thin film nanocomposites at 0, 2 and 4% doping ratios are illustrated in Fig (4a) in the wavelength range of 190-11000 nm. These spectra indicated a gradual decrease in the absorbance values with increasing wavelength, which is the behavior of semiconducting SnO_2 films. The absorbance diminished as the concentration of Cu dopant in the SnO_2 lattice increased. The absorption of light by Sn^{4+} ions was inhibited by the presence of Cu^{2+} impurity centers. The presence of Cu^{+2} induced defects in the crystal lattice of the storage material, consequently redistributing the atomic orbitals. The abundance of free electrons, characterized by high mobility, diminished the amount of electrons at the ground state, thereby leading to a reduction in the absorbance of materials [23,24].

The bandgap energy (E_g) of the prepared samples (pure SnO_2, SnO_2:0.02 Cu and SnO_2:0.04 Cu) was determined using Tauc's model:

$$(\alpha h\nu)^n = A(h\nu - E_g) \qquad (2)$$

where α, hν, E_g, n, and A represent the absorption coefficient, incident photon energy, energy gap, the exponent n (which varies based on the type of energy transition, e.g., n=2 for an indirect bandgap), and the proportionality constant, respectively [25]

In Fig. (4b), the synthesized pure SnO_2 exhibits a band gap of 3.021 eV, which increases with higher concentrations of copper, reaching 3.241 eV for the SnO_2:0.02 Cu sample and 3.283 eV for the SnO_2:0.04 Cu sample. This notable increase in band gap with Cu nanoparticles concentration is attributed to the quantum confinement effect. When ratio Cu increases, below band absorption transpires. As the concentration of Cu rises, the Urbach energy correspondingly increases, indicating a rise in distortion. The rise in distortion may result from two factors; either copper is generating levels adjacent to the conduction band, or the inclusion of copper into the system is creating oxygen vacancies that produce levels near the conduction band [26].

Gas sensors for NO_2 gas based on nanocomposites SnO_2:Cu have been fabricated, was examined at three temperatures (50, 100, and 150°C) at a constant flow rate of NO_2 gas by measuring the resistance (R MΩ) over time across two multi-finger electrodes. The transient response of the NO_2 gas sensor utilizing SnO_2:Cu is illustrated in Fig. (5). Three cycles were consecutively documented throughout measurement duration of 100 s. These cycles were documented in relation to various ultra-three temperatures of NO_2 gas. The reaction of SnO_2 to NO_2 gas was significantly influenced by surface shape. The sensor response (S%) is calculated by equation [27]:

$$S\% = \frac{R_a - R_g}{R_a} \times 100\% \quad (3)$$

where R_a represents resistance in the air and R_g represents the resistance when gas is released

The resistance of the SnO_2-based sensor escalated following exposure to NO_2 gas, with a rapid increase in response until maximum values were attained, as illustrated in Figures. Upon substituting NO_2 gas with air, the sensor resistance reverted to its original state, signifying a reversible adsorption of NO_2 molecules on the SnO_2 surface. The sensor's response to NO_2 gas exhibits a distinct increase as the temperature rises from 50 to 150 °C.

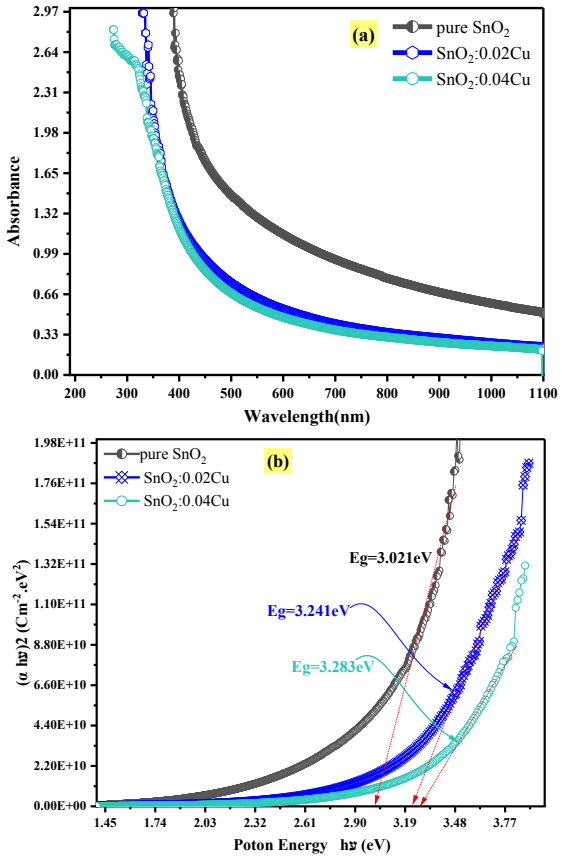

Fig. (4) (a) UV–visible absorption spectra and (b) energy gap plots of pure SnO_2, SnO_2:0.02 Cu and SnO_2:0.04 Cu

The sensitivity of NO_2 gas at working temperatures. The dynamic sensing transients of sensor upon exposure of NO_2 gas When the operating temperature increased, there was an increase in sensitivity within the range of S=4.1 to 8% for the three degrees reported above and referred to in table (2). As the temperature rises, the activity of the adsorbed gas molecules intensifies, leading to heightened interactions that amplify the variation in the film's electrical resistance. The acceleration of chemical processes enhances the efficiency of the contact between the poisonous gas and the sensitive surface, resulting in a significant alteration in electrical resistance, hence increasing sensitivity [28,29]. An improvement in the response of the SnO_2-based gas sensor was observed when the structure was enhanced by adding copper nanoparticles at percentages of 2 and 4% by weight. The sensitivity of the SnO_2:0.02 Cu film when gas opened was about 6.7% at 50 °C, and it increased to a value of 10.4% at 150 °C. While the improvement was noted for the SnO_2:0.04 Cu film over its predecessor, from ~11.4% to 105% at 150°C, with an improvement in response and recovery times.

Table (2) Response time, recovery time and gas sensitivity of gas sensors at operating temperatures of 50, 100 and 150 °C

Samples	T (°C)	Response Time (s)	Recovery Time (s)	Sensitivity (%)
Pure SnO_2	50	10.40	11.28	4.1
	100	10.40	11.57	4.7
	150	9.66	16.19	8.1
SnO_2:0.02 Cu	50	6.69	18.16	6.7
	100	9.75	14.64	7.9
	150	8.09	13.72	10.4
SnO_2:0.04 Cu	50	12.52	17.50	11.4
	100	10.41	17.81	9.6
	150	5.84	16.00	105

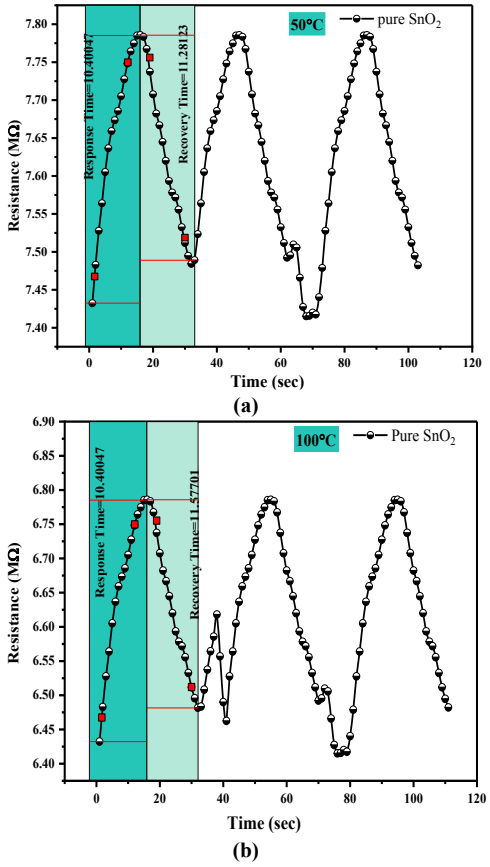

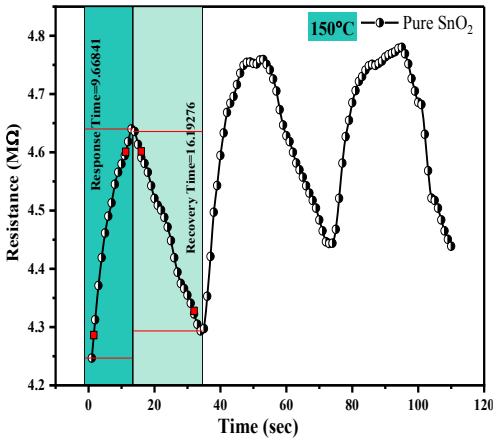

(c)

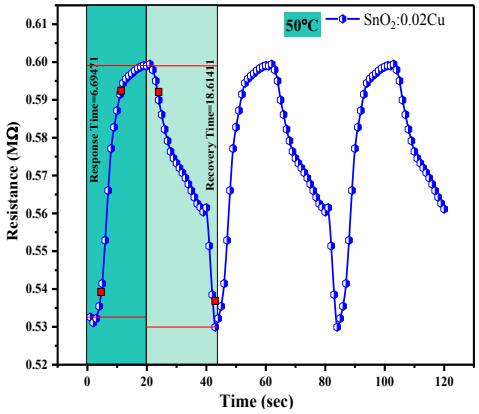

(d)

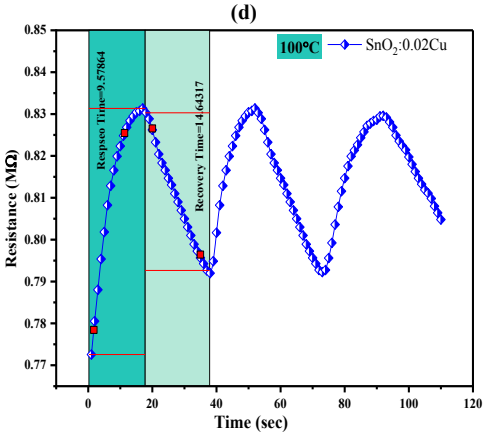

(e)

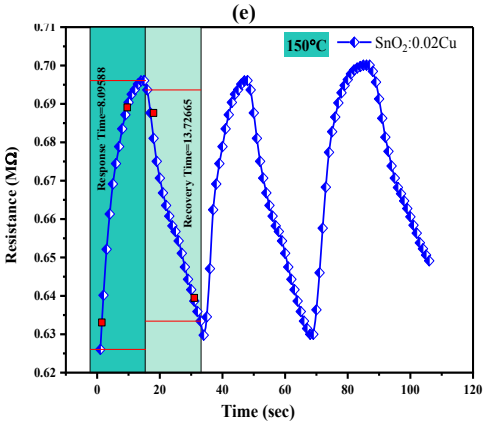

(f)

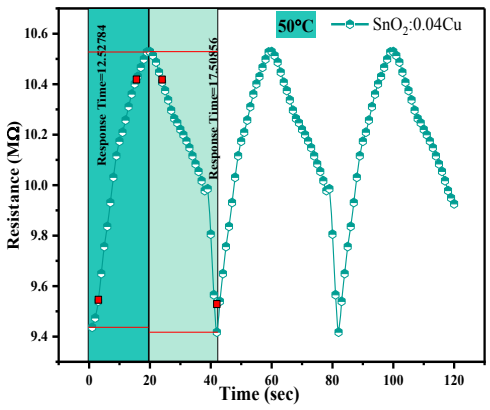

(g)

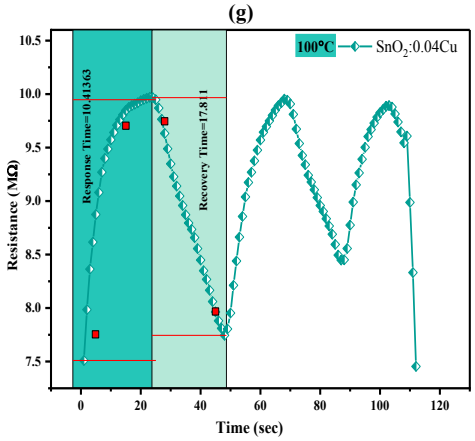

(h)

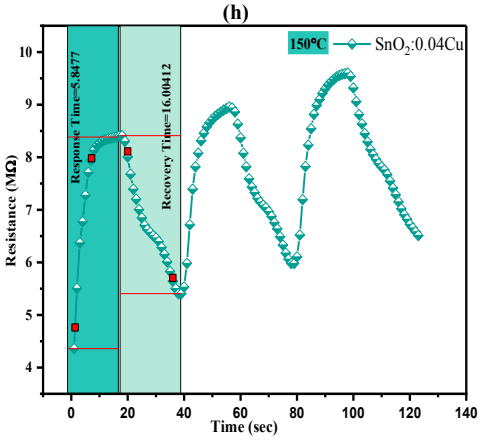

(i)

Fig. (5) (a-c) Response time of pure SnO_2 sample at 50°C, 100°C, 150°C, (d-f) for SnO_2:0.02 Cu sample at 50, 100, 150°C, (g-i) for SnO_2:0.04 Cu sample at 50°C, 100°C, 150°C

The inclusion of volume dopants can substantially affect sensing performance through many interaction aspects. The parameters can be categorized into four fundamental aspects: microstructure, encompassing dimensions (grain size), morphology, and crystallography; composition, which includes elemental composition, surface potential, free charge carriers, and electron exchange rates; catalysis, comprising catalytic activity, active phase, catalyst stabilization, and adsorption/desorption energy; and electrical properties, involving conductivity, surface

potential, free charge carriers, and electron exchange rates . The dopants can boost sensor qualities through the production and stabilization of smaller grains, the increase of nanostructure porosity, and the improvement of long-term stability [30,31,33]. Nonetheless, the development of an optimal sensor material continues to be problematic, as the enhancement of a beneficial attribute may concurrently impair another or exacerbate a detrimental characteristic**.**

4. Conclusion

The incorporation of copper nanoparticles into the tin oxide (SnO_2) structure showed an improvement in the structural, optical and gas detection properties of SnO_2 films deposited using the chemical spray deposition technique. The incorporation of copper at 2% or 4% enhanced the crystallinity of the films. The absorbance value decreased, while the energy gap increased from 3.02 to 3.28 eV. The fabricated NO_2 gas sensors showed a significant improvement at ratio SnO_2-0.04 Cu, achieving the highest response of 105% at an operating temperature of 150°C.

References

[1] N. Parvatikar et al., "Electrical and humidity sensing properties of polyaniline/WO_3 composites", *Sens. Actuat. B: Chem.,* 114 (2006) 599-603.

[2] L. Zhou et al., "High-performance humidity sensor based on graphitic carbon nitride/polyethylene oxide and construction of sensor array for non-contact humidity detection", *Sens. Actuat. B: Chem.,* 344 (2021) 130219.

[3] R. Kumar et al., "Exploring the possibility of using MWCNTs sheets as an electrode for flexible room temperature NO_2 detection", *Superlatt. Microstruct.,* 164 (2022) 107165.

[4] A.A. Hussain and Q.N. Abdullah, "Characterization of ZnO-SnO_2 Nanostructures Prepared by Thermal Evaporation Technique as Gas Sensor", *Iraqi J. Appl. Phys.,* 19(4C) (2023) 243-250.

[5] S. Sikarwar et al., "Fabrication of nanostructured yttria stabilised zirconia multilayered films and their optical humidity sensing capabilities based on transmission", *Sens. Actuat. B: Chem.,* 232 (2016) 283-291.

[6] V.N. Singh et al., "Size-dependent gas sensing properties of indium oxide nanoparticle layers", *J. Nanosci. Nanotech.,* 7 (2007) 1930-1934.

[7] J. Saura, "Gas-sensing properties of SnO_2 pyrolytic films subjected to UV radiation", *Sens. Actuat. B: Chem.,* 17 (1994) 211-214.

[8] M. Law et al., "Photochemical sensing of NO_2 with SnO_2 nanoribbon nanosensors at room temperature", *Angew. Chem. Int.,* 41 (2002) 2405–2408.

[9] K. Anothainart et al., "Light enhanced NO_2 gas sensing with tin oxide at room temperature: conductance and work function measurements", *Sens. Actuat. B: Chem.,* 93 (2003) 580-584.

[10] T.-Y. Yang et al., "UV enhancement of the gas sensing properties of nano-TiO_2", *Rev. Adv. Mater. Sci.*, 4 (2003) 48–54.

[11] S. Mishra et al., "Detection mechanism of metal oxide gas sensor under UV radiation", *Sens. Actuat. B*: Chem., 97 (2004) 387–390.

[12] E. Comini et al., "SnO_2 RGTO UV activation for CO monitoring", *IEEE Sens. J.,* 4 (2004) 17-20.

[13] C. Malagu et al., "Photo-Induced Unpinning of Fermi Level in WO_3", *Sensors*, 5 (2005) 594-603.

[14] C.-H. Wan et al., "Catalytic combustion type hydrogen gas sensor using TiO_2 and UV-LED", *Sens. Actuat. B*: Chem., 125 (2007) 224–228.

[15] Q. Wan, E.N. Dattoli and W. Lu, "Transparent metallic Sbdoped SnO_2 nanowires", *Appl. Phys. Lett.*, 90(22) (2007) 222107.

[16] J.J. Chen et al., "Interfacial Nanostructuring of ZnO Nanoparticles by Fullerene Surface Functionalization for "Annealing-Free" Hybrid Bulk Heterojunction Solar Cells", *J. Phys. Chem. C*, 116 (2012) 10841.

[17] X.H. Hou et al., "Preparation and electrochemical characterization of Zn_2SnO_4 as anode materials for lithium ion batteries", *Solid state Ionics*, 181 (2010) 631634-.

[18] D. Chen et al., "Electric transport, reversible wettability and chemical sensing of single-crystalline zigzag Zn_2SnO_4 nanowires", *J. Mater. Chem.*, 21 (2011) 17236.

[19] A. Zheng et al., "Peroxidase-like catalytic activity of copper ions and its application for highly sensitive detection of glypican-3", *Anal. Chim. Acta*, 941 (2016) 87-93.

[20] M.B. Gawande et al., "Cu and cu-based nanoparticles: Synthesis and applications in catalysis", *Chem. Rev.*, 116 (2016) 3722–3811.

[21] A.L. Patterson, "The Scherrer formula for X-ray particle size determination", *Phys. Rev.*, 56(10) (1939) 978.

[22] K. Kavitha, T. Subba Rao and R. Padmasuvarna, "Structural and Optical Characteristics of Cu Doped SnO_2 Nanostructures", *J. Nanosci. Nanotech. Appl.*, 1 (2017) 102.

[23] D.D. Toloman et al., "Enhanced photocatalytic activity of Co doped SnO_2 nanoparticles by controlling the oxygen vacancy states", *Opt. Mater.*, 110 (2020) 110472.

[24] T. Entradas et al., "Synthesis of sub-5 nm Co-doped SnO_2 nanoparticles and their structural, microstructural, optical and photocatalytic properties", *Mater. Chem. Phys.*, 147(3) (2014) 563-571.

[25] J. Tauc and A. Menth, "States in the gap", *J. Non-cryst. Solids,* 8 (1972) 569-585.

[26] V.S. Jahnavi, S.K. Tripathy and A.V.N.

Ramalingeswara Rao, "Study of the structural, optical, dielectric and magnetic properties of copper-doped SnO_2 nanoparticles", *J. Electron. Mater.*, 49(6) (2020) 3540-3554.
[27] N. Yamazoe and K. Shimanoe, "Theory of power laws for semiconductor gas sensors", *Sens. Actuat. B: Chem.,* 128(2) (2008) 566-573.
[28] R. Ramanathan et al., "A highly sensitive and room temperature ethanol gas sensor based on spray deposited Sb doped SnO_2 thin films", *Mater. Adv.*, 5(1) (2024) 293-305.
[29] R. Kumar et al., "SnO_2-based NO_2 gas sensor with outstanding sensing performance at room temperature", *Micromachin.*, 14(4) (2023) 728.
[30] K. Balasubramanian and M. Burghard, "Chemically functionalized carbon nanotubes", *Small,* 1(2) (2005) 180-192.
[31] S.R. Morrison, "Selectivity in semiconductor gas sensors", *Sens. Actuat.*, 12(4) (1987) 425-440.
[32] M.A. Carpenter, S. Mathur and A. Kolmakov (eds.), "Metal oxide nanomaterials for chemical sensors", Springer Science & Business Media (2012).

Table (1) Some structural parameters from XRD data

Sample	2θ (deg)	d(Å)	Intensity	FWHM (deg)	(hkl)	Crystallin size (nm)	Average Crystallin size (nm)
SnO_2 pure	26.31	3.38	184.5555	0.5904	110	13.09	10.79
	33.60	2.66	65.84702	0.984	101	7.72	
	37.77	2.38	127.4064	0.7872	200	9.54	
	51.67	1.76	107.7891	0.5904	211	12.10	
	61.92	1.49	33.47593	0.5904	310	11.53	
SnO_2:0.02Cu	26.49	3.36	839.2017	0.393	110	19.63	14.78
	33.47	2.60	339.935	0.492	210	15.45	
	37.182	2.35	197.4313	0.7872	200	9.561	
	52.334	1.74	342.6136	0.492	211	14.48	
SnO_2:0.04Cu	26.54	3.35	907.1252	0.688	110	11.23	14.67
	33.801	2.59	258.9784	0.393	210	19.33	
	38.418	2.34	461.0662	0.3936	200	19.05	
	51.72	1.75	361.0776	0.787	211	9.08	

